

Spatial distribution patterns of microbiome and nematodes in response to sediment ecological conditions

Soraia Vieira

Kasia Sroczyńska

Joana Neves

Marta Martins

Maria Helena Costa

Helena Adão

Claudia Vicente (✉ cvicente@uevora.pt)

University of Evora <https://orcid.org/0000-0002-3865-5358>

Research Article

Keywords: Sado estuary, microbiome, benthic nematodes, metagenomics

Posted Date: April 11th, 2022

DOI: <https://doi.org/10.21203/rs.3.rs-1525374/v1>

License:  This work is licensed under a Creative Commons Attribution 4.0 International License.

[Read Full License](#)

1 **Spatial distribution patterns of microbiome and nematodes in response to**
2 **sediment ecological conditions**

3
4 Soraia Vieira¹, Kasia Sroczyńska¹, Joana Neves², Marta Martins², Maria Helena Costa², Helena
5 Adão¹ and Cláudia S. L. Vicente³

6 ¹MARE – Marine and Environmental Sciences Centre, University of Évora, School of Sciences and
7 Technology, Apartado 94, 7002-554, Évora, Portugal

8 ²MARE – Marine and Environmental Sciences Centre, Department of Environmental Sciences and
9 Engineering, NOVA School of Science and Technology (FCT NOVA), 2829-516 Caparica, Portugal.

10 ³MED – Mediterranean Institute for Agriculture, Environment and Development, Instituto de Investigação
11 e Formação Avançada, University of Évora, Pólo da Mitra, Ap. 94, 7006-554 Évora, Portugal.

12
13 Corresponding author: cvicente@uevora.pt
14

15 **Abstract**

16 Benthic organisms are crucial in the regulation of the ecosystem functions. They are primary mediators of
17 the energy transfer in marine benthic food webs. Trophic interactions between benthic nematodes and
18 sediment bacteria across divergent environmental conditions are poorly understood. The main goal of this
19 study was to comprehend the relation between the spatial distribution patterns and diversity of benthic
20 microbial communities and nematode assemblages of the intertidal sediments in Sado estuary (SW,
21 Portugal). Samples were taken from three sites with different biogeochemical sediment conditions.
22 Microbial communities were described using metagenomic approach, while nematode assemblages were
23 characterized using morphological identification. Bacterial communities and nematodes assemblages
24 presented significant heterogeneity between sites ($p < 0.05$), which were primary related with the
25 environmental variables (e.g., organic matter deposits and gravel percentage). However, while microbiome
26 distributional patterns were clearly in accordance with ecological conditions of three selected sites (adjusted
27 $R^2_{Adj} = 0.53$), nematode assemblages were more responsive to specific sampling locations within each
28 site, suggesting that their response is rather driven by the within site specific factors, acting at the smaller
29 spatial scale. Our study also demonstrated that the presence of Cyanobacteria (higher relative abundance
30 of *Pleurocapsa* PCC-7319) seemed to be correlated with high abundance of nematode deposit feeders

31 *Terschellingia* and *Sabatieria* indicating possible interactions between these taxa. Our study represents a
32 first insight into bacteria–nematodes associations underlying ecological conditions thereby providing an
33 important baseline for the future understanding of the role that these two groups play in the benthic estuarine
34 ecosystem.

35

36 **Keywords:** Sado estuary, microbiome, benthic nematodes, metagenomics

37

38 **Introduction**

39 Estuarine and coastal benthic ecosystems represent one of the major sources of essential services for
40 human well-being [1, 2]. They play a crucial role in regulating fundamental ecosystem functions such as:
41 food production, degradation and distribution of pollutants, recycling of nutrients and transfer energy
42 through trophic processes [2]. These functions are mediated by intra and interspecific interactions between
43 organisms that support the functional integrity of the benthic ecosystems [3].

44 Benthic nematodes represent 50-90% of biomass in shallow sediments [4] and are considered an
45 important tool to assess the effects of natural and anthropogenic disturbances in marine and estuarine
46 sediments [5, 6]. These organisms also play important roles in several ecosystem processes, being involved
47 in complex relationships with microbial communities [1, 7]. Their buccal cavity morphology only allows
48 the ingestion of a restrict type of food (e.g., bacteria or detritus) affecting the abundance and activity of the
49 microbial communities [7, 8]. Furthermore, nematode activities related with bioturbation, extracellular
50 polymeric substances (EPS) production and grazing have been proved to be an important contribute to
51 stimulate the microbial development and growth [9–11]. Nematodes are thus important mediators of energy
52 transfer to higher trophic levels [12–14], while sediment microbes are the primary facilitators of
53 biogeochemical processes, such as carbon remineralization and sulphate reduction [15, 16]. A strong
54 interconnection between nematode-microbe communities is well recognized, the presence of nematodes
55 enhances microbial metabolic activities, while bacteria provide physiological adaptations to nematodes
56 under hypoxic and anoxic conditions [8, 17, 18].

57 Assessing ecosystem conditions become one of the majors concerns over the past two decades.
58 Majority of the studies have been focused on the analysis of a single taxonomic group distribution patterns
59 and relate with ecosystem environmental parameters [19–21]. However, such approach does not consider
60 the interaction between organisms belonging to different taxonomic entities, thereby limiting the
61 assessment of the functional component of the ecosystem. The existence of the above-mentioned
62 associations between bacteria and nematodes, still it is largely unknown how both groups interact in the
63 context of community distributional patterns and most importantly if exists any congruence between both
64 groups in their response to ecological conditions. Applying the novel high performance methodological
65 approaches such as metagenomics to analyse the sediment microbiome diversity provide the possibility to
66 develop essential understanding of the connection between benthic organisms. The main goal of this study
67 was to understand the relation between the spatial distribution patterns and diversity of benthic microbial

68 communities and nematode assemblages of the intertidal sediments in Sado estuary in Portugal. The
69 diversity patterns were investigated using: *i*) a metagenomic approach for microbial communities'
70 assessment; and *ii*) a morphological approach for the characterization of nematode assemblages. The
71 sediment biogeochemical conditions were analysed to assess the ecological conditions at each sampling
72 site. Drawing from above it is hypothesized that spatial distribution patterns of microbial communities will
73 follow the same patterns as spatial distribution of nematode assemblages, both responding to the
74 biogeochemical variables of the estuary in a similar way.

75 **Experimental Procedures**

76 **Study area and sampling design**

77 The Sado estuary is the second largest estuarine system in Portugal, with an area of approximately
78 240 km², being one of the most important wetlands in Europe [22] (Fig. 1). The intertidal areas comprise
79 approximately 78 km², of which 30% are salt marshes and intertidal flats [23]. Sado estuary has a semi-
80 diurnal mesotidal system with tidal amplitude varying between 0.6 m and 1.6 m during spring and neap
81 tides, respectively. Salinity is influenced by the Sado river flow (annual mean of 40m³.s⁻¹) changing with
82 seasonal and inter-annual conditions and temperature can range from 10 to 26°C.

83 The sampling sites were selected based on the expected differences in biogeochemical and trophic
84 conditions of the sediments according to water hydrodynamics within an estuary (high/low water residence
85 time), salinity gradient and the type of neighboring anthropogenic activities [24–26]. Based on above-
86 mentioned criteria three “Sampling Sites” were selected: (1) Navigator Site located in the proximity of
87 industrial area (Fig. 1). Main sediment fractions are dominated by fine sand and clay, with the high organic
88 matter content while dissolved oxygen levels are reduced [27]; (2) Moinho Site is located within the borders
89 of the Sado Nature Reserve, directly affected by the surrounding aquaculture activities. The aquaculture
90 exploitation are the main contributors for the substantial high organic matter deposits, low dissolved oxygen
91 concentrations levels and predominance of clay-like sediments [26]; (3) Tróia Site is located close to the
92 estuary mouth, is directly exposed to the main estuary channel, contributing to high water exchange rate,
93 high dissolved oxygen concentration levels and high proportion of the coarse type sediment (*e.g.*, sand)
94 [26].

95 At each “Sampling Site”, three sediment replicates were randomly collected at neap low tide to
96 investigate microbiome communities, benthic nematodes assemblages, and measured environmental
97 variables. The sediment physical-chemical composition was obtained analysing the granulometry (%)

98 (gravel, sand, and FF), elemental contents (W%) (OM, TN and TC, IN IC) and salinity (Supporting
99 information Table S5).

100 **Sample processing of benthic communities**

101 *Total DNA extraction of sediment and amplicon sequencing*

102 Samples were taken from sediment surface at 10 cm depth into a sterilized 50-mL Falcon Tube,
103 snap-frozen in dry ice and transported into the lab, where were stored at -80°C until DNA extraction. Total
104 DNA extraction from 0.25 g of the sediment was conducted under sterile conditions, using the MOBIO
105 PowerSoil® kit (QIAGEN, Valencia, CA, USA) following the manufacturer's instructions. For cell lysis,
106 samples were homogenized in a Precellys 24 Tissue Homogenizer (Bertin Instruments) for a total of 6
107 minutes (2x 20'' at 5000 rpm). The quality and quantity of total DNA was analysed through
108 NanoDrop™2000 Spectrophotometer (Thermo Fisher) and Qubit4® fluorometer (Thermo Fisher
109 Scientific). The presence of amplifiable DNA was confirmed by amplicon amplification with primers
110 flanking the V4 region of 16S rRNA (515F–806R)[28]. A total of 9 samples were selected and sent for
111 sequencing on Illumina MiSeq 2x 250bp (Illumina, Inc. San Diego, CA, USA) at EUROFINs Genomics
112 (Cologne, Germany).

113

114 *Bioinformatics analyses and data availability*

115 Raw Illumina data was demultiplexed and quality-filtered using the defaults parameters of
116 QIIME2 [29]. Single-end read data were denoised using DADA2 [30] plugin, that discarded biased reads
117 (e.g., chimeras, singletons) and determined the amplicon sequence variants (ASVs). Further, ASVs were
118 clustered into Operational Taxonomic Units (OTUs) at 97% similarity using VSEARCH open-reference
119 OTU picking strategy against the SILVA v138 reference database [31]. Representative sequences were
120 assigned taxonomy using a trained Naïve Bayes classifier (SILVA 138) [32] for V3-V4 hyper variable
121 region from 16S rRNA. The resulting OTUs table was filtered to keep only features with a total abundance
122 less than 10. OTUs classified as chloroplast, mitochondria, eukaryote, archaea, and unassigned were also
123 removed. Filtered OTUs table was rarefied at 14000 sequences per sample after confirmation with
124 rarefaction plugin. Raw data supporting our results have been deposited into the NCBI SRA repository
125 under the Bioproject PRJNA680980 and accessions SRR13151077-13151079 (NAV), SRR13165305-
126 13165307 (TRO), and SRR13165323- SRR13165325 (MOI).

127 *Nematode assemblages*

128 Nematode samples were collected at each sampling site by forcing a hand core (3.8 cm inner
129 diameter) to a depth of 3 cm into sediment. Each replicate was fixed in a 4% buffered formalin. Each sample
130 was first rinsed on a 1000 μm mesh sieve and then on a 38 μm mesh sieve. Nematodes were extracted from
131 sediment using LUDOX HS-40 colloidal silica at specific gravity 1.18 g cm^{-3} [33]. Nematodes were counted
132 using a stereomicroscope Leica M205 (100x magnification) and a counting dish. From each replicate, a
133 random set of 120 nematodes was picked, transferred through a graded series of glycerol-ethanol solutions,
134 stored in anhydrous glycerol, and mounted on slides for further identification [34]. Based on morphological
135 characters, each nematode was identified until genus level (Olympus BX50 light microscope and cell
136 software D Olympus, Japan). Identification was made using pictorial keys [35, 36], and online identification
137 keys/literature available in the Nemys database [37].

138 **Statistical analyses**

139 The statistical analyses of the nematode assemblages and environmental data was performed using
140 the PRIMER v6 software package [38] with permutational analysis of variance (PERMANOVA) add-on
141 package [39]. Statistical analyses of 16S rRNA metagenomics was performed in Quantitative Insights into
142 Microbial Ecology (QIIME2, version 2020.8) [29] and *phyloseq* R package [40].

143 *Environmental factors*

144 Environmental data was analysed using PCA. The analysis was applied to a data matrix based on
145 three replicates from each “site” to explore patterns in multidimensional data. Data were $\log(X + 1)$
146 transformed (OM, %gravel and FF) and normalized [38]. The redundant variables were removed from the
147 analysis (TN, TC and NO) and variables retained in the model acted as proxy for the ones that were
148 eliminated (OM, gravel, sand, FF, IN, IC, CO and Sal).

149

150 *Environmental factors influencing the communities*

151 Redundancy Analysis (RDA) was conducted to test linear combinations of the environmental
152 variables that best explain the variation of the microbial and nematode communities' patterns. The response
153 dataset consisted of Hellinger-transformed relative microbial (observed OTUs with taxonomy assignment,
154 corresponding to the 20 most abundant taxa) matrix, nematode genera abundance matrix [41] and
155 explanatory environmental data. Variation inflation factors (VIF) were calculated to check for linear
156 dependencies and to ensure that only variables with small VIFs (<10) were included. These were: “OM”,
157 “Gravel %”, “FF_p”, “IN_wp”, “IC_wp” and “Sal”. All the variables were transformed using arcsine

158 square root transformation, except for salinity that was log₁₀ transformed. A forward selection procedure,
159 using function ordiR2step() was used to select only significant variables ($p < 0.05$) . RDA analysis was
160 performed in R [42] using “vegan” and “BiodiversityR” packages [43]. To test the correlation between both
161 ordinations (microbiome and nematodes) it was performed Pro- crustean test [44]. Procrustean test
162 measures the degree of concordance between two or more datasets having different characteristics and if
163 statistically significant, two datasets reflect in the same way the processes that determine their association
164 [45].

165 *Microbial communities*

166 α - and β -diversity indexes were calculated with q2-diversity plugin. For α -diversity analysis,
167 several descriptors were determined: Observed, Chao1, Shannon, Simpson and Pielou’s Evenness. The
168 Kruskal-Wallis test, $p < 0.05$ and Kruskal-Wallis (pairwise), were performed to determine the α -diversity
169 significance (within sites) for all groups and one-way PERMANOVA was performed to test null hypothesis
170 that no spatial significant differences between sites (β -diversity significance), $p < 0.05$. The similarity of
171 microbial communities’ composition in “Sites” were plotted by Principal Coordinates Analysis (PCO)
172 using the Bray-Curtis similarity. The relative contribution of each taxon to the dissimilarities between sites
173 was calculated using the two way-crossed similarity percentage analysis SIMPER (cut-off percentage
174 100%).

175 *Nematode assemblages*

176 Benthic nematode assemblages were characterized using the following parameters: total density
177 (individuals per 10 cm⁻²) of the nematodes, genera, trophic composition and structural diversity (*e.g.*,
178 Margalef’s richness Index (d) [46] and Shannon Wiener diversity (H₀) [47]. Indicators based on ecological
179 strategies were also calculated: Index of Trophic Diversity (ITD) [33] and Maturity Index (MI) [48, 49].
180 To assess the trophic composition of the assemblages, feeding groups based on mouth morphology were
181 assigned to every nematode genus [50], and the ITD was calculated [33]. The reciprocal index (ITD⁻¹)
182 shows that the higher value of ITD⁻¹ corresponds to the higher trophic diversity. The MI was used as a life
183 strategy measure, in which a value on a colonizer-persister scale (*c-p* scale) from 1 (colonizers) to 4
184 (persisters) was assigned to each genus. One-way PERMANOVA was performed to the assemblage
185 descriptors (number of genera, d, H, Trophic composition, ITD⁻¹ and MI indices) to test the null hypothesis,
186 no significant differences of the density, diversity and trophic composition of the nematode were detected
187 between “Sites”.

188 The PERMANOVA analysis were carried out with a one factor design: “Site”: “Moinho”;
189 “Navigator”; “Tróia” (3 levels, fixed) using a Bray-Curtis similarity matrix [38], $p < 0.05$. The similarity of
190 microbial and nematode communities’ composition in “Sites” were plotted by Principal Coordinates
191 Analysis (PCO) using the Bray-Curtis similarity measured. The relative contribution of each taxon to the
192 dissimilarities between sites was calculated using the two way-crossed similarity percentage analysis
193 SIMPER (cut-off percentage 100%).

194 **Results**

195 **Environmental variables**

196 The sampling area is delimited within the Sado estuary in three sampling sites – Moinho, Navigator
197 and Tróia (Fig.1). The environmental variables measured in sediment and water in each site revealed
198 contrasting conditions (Supplemental material Table S1) supporting a clear separation in the PCA (Principal
199 Component Analysis) (PC1: 59.2% and PC2:31.4%) (Fig. 2). The spatial distribution patterns detected were
200 mainly due to the highest values of sediment Organic Matter (OM), Organic Carbon (OC), Inorganic
201 Nitrogen (IN) and Fine Fraction (FF) at Moinho site and the highest proportion of Gravel, Sand and Salinity
202 (Sal) in Navigator and Tróia sites (Fig.2).

203 **Bacterial communities**

204 *Sequencing statistics, diversity, and richness estimations*

205 Illumina sequencing of the nine sediment samples (Navigator, NAVR1-R3; Tróia, TROIAR1-R3;
206 and Moinho, MOIR1-R3) yielded a total of 435.781 sequence reads, out of which 175.796 high-quality V3-
207 V4 16S rRNA sequence reads were clustered into 1.683 OTUs. For each sample, 15.000 reads were
208 considered for further analysis after rarefaction (Supporting information Fig. S1). The observed OTUs were
209 in accordance with Chao1 descriptor, obtained in all sites the following values: NAVR1-R3 (448-575),
210 MOIR1-R3 (375-500) and TROIAR1-R3 (344-521) (Table S2). All sampling sites showed a high richness
211 and diversity with Shannon index ranging between 7.8 (TROIAR3) and 8.56 (NAVR2), while Simpson
212 Index and evenness were nearly 1. Further consideration of the α -diversity patterns, no significant
213 differences ($p > 0.05$) were obtained between bacterial taxa in each site nor between replicates within each
214 site ($p > 0.05$) (Table S3). In terms of β -diversity, based on PERMANOVA calculated at OTU level revealed
215 a significant clustering of samples within the ordination space (between “Sites”, $p < 0.05$) (Table 1). The
216 PCO showed a clear separation of bacterial community from Navigator site from other two sites (Moinho

217 and Tróia) (PC1 30.4% and PC2 17.5%) accounting together for app. 50% of the variability in the bacterial
218 communities (Fig. 3).

219 *Bacterial composition differences across sites*

220 Bacterial communities from all sites are composed by 53 phyla from which 18 were the most
221 representative, accounting for more than 90% of the taxa with more than 1% of the communities' total
222 abundance (Fig. 4). The most abundant phyla were: Proteobacteria (38-42%), Desulfobacterota (20-23%),
223 Chloroflexi (5-9%), Bacteroidota (5-6%) and Acidobacteriota (2%). In Moinho site, the bacterial
224 community was composed by 247 genera from 269 families. The most abundant taxa belonged to the classes
225 Gammaproteobacteria (38 genera), Alphaproteobacteria (30 genera), Bacteroidia (23 genera),
226 Desulfobacteria (11 genera), Cyanobacteriia (8 genera), Anaerolineae (8 genera) and Desulfobulbia (7
227 genera). Within the most abundant classes (Gammaproteobacteria, Desulfobacteria and Desulfobulbia), the
228 most representative orders were Steroidobacterales, Gammaproteobacteria_incertae_Sedis, Chromatiales,
229 Desulfobulbales and Desulfobacterales, which were mainly represented by the families Woeseiaceae,
230 Desulfobulbaceae and Desulfosarcinaceae, accounting for more than 20% of total abundance (Fig. S2). The
231 most abundant genera were *Woeseia* (8.1-10.8%), *Sva0081_sediment_group* (4.3-5.6%), *Sva1033* (3.6-
232 3.7%), *B2M28* (1.9-2.8%) and *Candidatus Thiobios* (1.6-2.5%).

233 In Navigator site, bacterial communities were composed by 321 genera and 306 families, whilst the
234 major number of genera belonged to the classes Gammaproteobacteria (52 genera), Alphaproteobacteria
235 (48 genera), Bacteroidia (31 genera), Desulfobacteria (10 genera) and Anaerolineae (10 genera). Within the
236 most abundant classes (Gammaproteobacteria, Desulfobacteria and Cyanobacteriia), the most
237 representative orders were Steroidobacterales, Desulfobacterales and Cyanobacteriales respectively
238 represented by the families Woeseiaceae, Desulfosarcinaceae, Desulfobulbaceae and Xenococcaceae (Fig.
239 S2). The dominant genera were *Woeseia* (8-9%), *Sva0081_sediment_group* (5.2-5.7%) and
240 *Pleurocapsa_PCC-7319* (0-4%), each one has a contribute >4% of the total density of the bacterial
241 communities collected in Navigator site. The phylum Cyanobacteria were exclusively represented in
242 abundance by the genera *Pleurocapsa_PCC-7319* at Navigator site. The Tróia bacterial community was
243 composed by 249 genera and 272 families, whereas the most abundant taxa belonged to the classes
244 Alphaproteobacteria (36 genera), Gammaproteobacteria (34 genera), Bacteroidia (26 genera),
245 Desulfobacteria (9 genera), Desulfobulbia (8 genera), Anaerolineae (11 genera), Cyanobacteriia (3 genera)
246 and Acidimicrobiia (4 genera). Within the most abundant classes (Gammaproteobacteria and

247 Desulfobacteria), the most representative orders were Steroidobacterales and Desulfobacterales
248 (Woeseiaceae and Desulfosarcinaceae families), counting more than 17% of total abundance of the
249 community (Fig. S2). The most representative genera of communities were *Woeseia* (6.9-8.1%),
250 *Sva0081_sediment_group* (3.7-7.3%), *SEEP-SRB1* (1.7-2.6%), *SBR1031* (1.8-3.7%) and *Sva1033* (2.7-
251 3.6%) each one corresponds to >1% of Tróia communities' total abundance.

252 The SIMPER analysis showed that bacterial taxa that most contributed for the similarity within
253 sampling sites were the *Woeseia*, *Sva0081_sediment_group* and *Sva1033* (Similarity ≥ 68 %). Moreover,
254 the great contributors for the major dissimilarities between sites were the genera *SEEP-SRB1* and *SBR1031*
255 (Moinho vs Tróia, dissimilarity 29.94%), *Pleurocapsa_PCC-7319*, *Myxosarcina_GII* and
256 *Cyanobacterium_CLG1* from the order Cyanobacterales (Moinho vs Navigator and Navigator vs Tróia,
257 dissimilarity 34-36%).

258 **Nematode assemblages**

259 *Density and structural diversity*

260 Overall, the nematode density varied between 2706.3 and 13466.9 individuals per 10 cm² (Table
261 2). The nematode assemblages of Moinho site registered the highest mean density (13466.9 \pm 1631.1 ind.
262 10 cm²), whilst the lowest mean density was obtained at Navigator sampling site (2706.4 \pm 1092 ind. 10
263 cm²). PERMANOVA analysis for the nematode density revealed significant differences between "Sites",
264 $p \leq 0.05$ (Table S4). Nematode assemblages' diversity was high in all sampling sites (Table S5). Nematode
265 richness based on Margalef Index (d) registered the highest value in "NAVR3" ($d=2.86$) and lowest values
266 was registered in "MOIR1" ($d=0.86$). Genera diversity based on Shannon-Wiener index (H') registered the
267 highest value at "NAVR3" ($H'=2.29$) and the lowest value at "MOIR1" ($H'=1.2$) (Table S5).
268 PERMANOVA analysis conducted based on structural diversity descriptors (d , H' ITD⁻¹ and MI)
269 demonstrated significant differences between "Sites", $p \leq 0.05$, only for Margalef richness (d) (Table S4).

270 The nematode assemblages collected in the Navigator site were composed by 29 nematode genera
271 belonging to 14 families. Most of the genera belonged to the orders Monhysterida (46.6%), Chromadorida
272 (26.8%) and Enoplida (6%) and the dominant families were Linhomoeidae (53.3%), Desmodoridae (15.9%)
273 and Comesomatidae (10.8%). The genera *Terschellingia* (52%), *Metachromadora* (15%), *Sabatieria* (9%)
274 and *Anoplostoma* (5%) represent 82% of the total density of the nematode assemblage collected in
275 Navigator (Fig. 5 and Fig. S3). The remaining 25 nematode genera accounted 18% of the total density. The
276 assemblages that accounted for the highest density values were from Moinho sampling site, they were

277 composed by 20 nematode genera belonging to 13 families. Most of the identified taxa belonged to the
278 orders Chromadorida (59.2 %), Monhysterida (20 %) and Enoplida (1.8%), being the dominant families
279 Desmodoridae (56.1%), Linhomoeidae (13.8%) and Comesomatidae (8.8%). *Metachromadora* (56%),
280 *Terschellingia* (14%), *Sabatieria* (7%) and *Axonolaimus* (5%) and they accounted for 84% of the Moinho
281 assemblages (Fig. 5 and Fig. S3). The nematodes identified at Tróia sampling site were composed of 20
282 genera from 12 families. Almost all genera belonged to the orders Chromadorida (42.5 %), Monhysterida
283 (12.3%) and Enoplida (2.5%) with the dominant families being Desmodoridae (56.1%), Linhomoeidae
284 (13.8%) and Comesomatidae (8.8%). The 4 dominant genera *Metachromadora* (49%), *Terschellingia*
285 (16%), *Ptycholaimellus* (7%) and *Sabatieria* (7%) represent 80% of the assemblages collected in Troia site
286 (Fig. 5 and Fig. S3).

287 The PCO ordination of the nematode assemblages showed a clear separation of Moinho site from
288 Navigator and Tróia sites. These results reflect high variability of nematode density between sites (PC1
289 40.9 % and PC2 25% contributions) together accounted for about 65.9 % of the total variability in the
290 density data (Fig. 6). Concerning this ordination, SIMPER analysis showed that *Metachromadora*
291 *Terschellingia*, *Sabatieria* and *Axonolaimus* were the genera that most contributed for the similarity within
292 sites, while *Metachromadora* *Terschellingia* and *Axonolaimus* were the genera that most contributed for
293 the dissimilarity between sites. Although the assemblages of Moinho and Navigator sampling sites were
294 clearly separated, the nematode community profiles showed distinct spatial distribution patterns comparing
295 to those obtained for the microbial communities.

296 *Trophic composition and Functional diversity*

297 Navigator assemblages were mainly characterized by selective deposit feeders (1A) and non-
298 selective deposit feeders (1B), representing 63% of the nematode assemblages. While 52% of the Moinho
299 assemblages were characterized by omnivores/predators (2B). Tróia nematode assemblages were mainly
300 comprised of omnivores/predators (2B: 45%) and selective deposit feeders (1A: 18%) (Table 2).
301 PERMANOVA analysis of the nematode trophic composition data revealed significant differences between
302 “Sites” ($p \leq 0.05$) (Table S4).

303 The Trophic diversity Index (ITD⁻¹) values ranged from 1.7 to 3 where the highest value was
304 obtained at Navigator site (varying from 2 to 3), corresponding to the highest trophic diversity between
305 assemblages of each site, while the lowest values (varying from 1.7 to 2.3) was registered in Moinho (Table
306 S5) besides the highest density values at this site. The maturity index (MI) varied from 2.1 to 2.7 and the

307 highest values were obtained in Navigator sampling site, while the lowest values were registered in Tróia.
308 These results revealed the colonizer strategy (*c-p* value 2) dominated at Moinho (57%) and Troia (42%).
309 Navigator sampling site was dominated (46%) by the genera classified as *c-p* value 3. PERMANOVA
310 analysis of the functional diversity descriptors revealed no significance differences between “Sites” ($p \leq$
311 0.05) (Table S4), highlighting the prevalence of similar trophic diversity and opportunistic strategies among
312 nematodes inhabiting all three sites.

313 **Environmental factors influencing both benthic communities**

314 The RDA ordination on microbial communities constrained by the environmental variables was
315 highly significant ($F = 5.44$, $p = 0.001$, adjusted $R^2_{Adj} = 0.53$) (Fig. 7A). The cumulative explained
316 proportion of both axes was remarkably high reaching 64.44%. The environmental variables that emerged
317 as significant were % Gravel ($p=0.045$) and % OM ($p=0.005$). According to triplot (Fig. 7 A), there was a
318 very clear separation of all sites, particularly Navigator with clear separation from Moinho and Tróia along
319 the first axis accounting for the highest proportion explained (56.27 %) of the total variability in community
320 data. High proportions of gravel in NAVR3 were correlated with the prevalence of Xenococcaceae family.
321 Desulfocapsaceae, Ilumatobacteraceae and BD2-11_terrestrial_group were associated to NAVR1 and
322 NAVR2. Moinho was characterized by high OM deposits with certain affinity of: Desulfobulbaceae,
323 B2M28, Chromatiaceae and Sva1033 families. Tróia sampling sites (TROIAR1-R3) were tightly grouped
324 together with strong affinity of SBR1031 and Desulfosarcinaceae families as well as Cyclobacteriaceae
325 (Fig. 7A).

326 The RDA ordination on nematode assemblages’ data constrained by the environmental variables was
327 highly significant ($F = 2.49$ $p = 0.001$, adjusted $R^2_{Adj} = 0.35$), with the first RDA axis explaining 32.82%
328 and the second explaining 19.91% of the variance in nematodes assemblage data (Fig. 7B). Significant
329 emerged environmental variables were: % Gravel ($p=0.035$), % OM ($p=0.015$) and inorganic carbon
330 ($p=0.010$). Similarly, as it was observed with microbiome communities Navigator was separated from the
331 remaining sites. This separation was driven by the high % Gravel content at NAVR2 and Inorganic Carbon
332 at NAVR1. Genera associated to NAVR2 included *Odontophora*, *Calyptronema*, *Aegialoalaimus* and
333 *Metalinhomoeus*, whereas *Terschellingia*, *Microlaimus*, *Camacolaimus* and *Spirina* were instead
334 associated to NAVR1. The presence of *Viscoccia* and *Paracomesoma* were highly related to NAVR3. On
335 the other hand, *Metachromadora* was demonstrated to yield clear affinity to TROIAR2 and MOIR1, while
336 the presence of *Axonolaimus* was highly correlated with MOIR2 and TROIAR3.

337 Besides microbial-based RDA had only two environmental variables significantly correlated with the
338 community ordination, its overall significance and remarkably high AdjRsquare indicates that only these
339 two variables were able to predict majority of the variability occurred in microbial community data.
340 Additionally, only 20 most abundant microbiome families were sufficient to clearly separate 3 distinct sites.
341 On the other hand, nematode assemblages were more responsive to specific sampling replicates within each
342 site. Organic matter and gravel were demonstrated to yield equal importance (yet exhibited in a different
343 way) for the distribution patterns of both bacterial and nematode groups. The result of Procrustes test that
344 analysed the correlation between both ordinations was not significant (Correlation in a symmetric
345 Procrustes rotation: 0.4897, $p=0.324$).

346 **Discussion**

347 The high spectrum of environmental conditions registered in estuarine sediments are well known
348 to capture a variety of adaptive responses in benthic communities [27]. In this study, the spatial distributions
349 of microbial and nematode communities were studied in three contrasting sites of Sado estuary. As initially
350 hypothesized, both benthic communities followed a consistent distribution pattern, being congruent with
351 the sediment biogeochemical conditions.

352 The influence of the environmental conditions on the spatial distribution patterns of the bacterial
353 communities is well known [51, 52]. At all sites, microbial communities were dominated by Proteobacteria
354 and Desulfobacteriota phyla, both known to play important roles in most of the biogeochemical processes
355 (e.g., anaerobic processes in sulfur and carbon cycles) in estuarine sediments [52–54]. The presence of
356 Woeseiaceae and Halieaceae families were also detected in all sampling sites, which is corroborated by
357 their wide occurrence and contribution to the biogeochemical processes in marine sediments [55, 56].
358 Symbiotic organisms from the family Rhodobacteraceae [11] and sulfur-oxidizing bacteria *Candidatus*
359 *Thiobios* were also detected in abundance in all sampling sites. These organisms are recognized to be
360 involved in symbiotic mechanisms with nematodes, providing them beneficial physiologic adaptations
361 (such as protection against adverse conditions) [17, 57, 58]. In the case of Moinho site, the high prevalence
362 of Desulfobulbaceae family may evidence the anoxic conditions of the sediments, since the metabolic
363 processes of these sulphate reducers are mainly involved in anaerobic degradation of organic matter [54,
364 59]. Cyanobacteria were responsible for separating bacterial communities of Navigator from the other sites,
365 with the exclusive presence of the unicellular and pseudo-filamentous genus *Pleurocapsa* [60]. These
366 organisms are regarded as ecological important group in estuarine and coastal environments being primary

367 producers and nitrogen/carbon fixators, and their increased grow highlight the presence of opportunistic
368 species with the release of cyanotoxins [60, 61]. The distribution patterns of bacterial communities at the
369 Navigator site, highlighted by the exclusive presence of cyanobacteria, are strictly related to the high
370 proportions of gravel and salinity, which is in accordance with Kolda [60], that showed the preference of
371 cyanobacteria for a sandy gravel type of sediment.

372 As for the nematode communities, their density was similar to those reported other Portuguese
373 estuaries (SW coast of Europe), such as Mira, Mondego and Sado estuaries [19, 27, 62] with the exception
374 of Moinho sampling site that diverged from others registering the highest nematode density. The highest
375 content of OM at this site could be related, since nematode density and distribution are highly related to the
376 food and OM available at the bottom of the sediments [9, 63]. The predominance of sandy sediments in
377 Navigator and Tróia sampling sites contributed to the low nematode density but a diversity increase,
378 possibly related with the broader range of microhabitats available for nematodes in these sediments when
379 compared to muddy ones [64]. In all sampling sites, the dominant genera were *Metachromadora*,
380 *Sabatieria*, *Axonolaimus* and *Terschellingia*, similar composition to mud-flat areas of Mondego estuary
381 [62] and also to the previous study in Sado estuary [27]. The spatial distribution patterns base on ITD⁻¹ and
382 MI indexes were also similar to those verified in Mondego, Mira and Sado estuaries [19, 27, 65]. However,
383 the trophic composition of nematode assemblages showed different results from previous studies (i.e.,
384 usually dominated by non-selective deposit feeders (1B) and epistrate feeders (2A) [20, 62]. The
385 omnivores/predators (2B) were dominant in all sampling sites, which are mainly grazers of
386 microphytobenthos and bacteria [66]. These organisms are usually able to vary their feeding mode in
387 response to the food availability being difficult to draw a general trend in abundance of these feeding groups
388 [9, 12]. Nematode communities sampled in Navigator showed a high percentage of non- and selective
389 deposit feeders (1A and 1B) such as *Terschellingia* and *Sabatieria*, which are usually favoured by the
390 depositional nature and hypoxic conditions of the sediment. Moreover, Vafeiadou [12] and Sahraean [67]
391 demonstrated by stable isotope analysis that *Terschellingia* can thrive under conditions that benefit the
392 chemoautotrophic prokaryotic activity (e.g., *Cyanobacteria*) by using methane-derived carbon as energy
393 source. Schuelke [68] did not find a clear distribution patterns of nematodes-associated microbiomes
394 between different geographical areas with different environmental conditions. However, the dataset did
395 reveal a variety of new ecological interactions, including putative symbionts and parasites as well as
396 associations with prokaryotic taxa involved in methane and nitrogen cycling. The type of nematode-bacteria

397 interaction is not possible to be defined by our results, yet the abundance of *Terschellingia* and
398 Cyanobacteria at Navigator sampling site may suggest a possible connection between benthonic organisms
399 considering the previous studies [12, 67].

400 **Concluding remarks**

401 Our study demonstrated that nematodes assemblages and microbiome communities respond
402 closely to the ecological conditions of the estuary. In fact, the RDA analysis showed that, for both benthic
403 communities, the OM and the %Gravel were the main contributors of their spatial distribution patterns in
404 two of the sampling sites. These findings yield great potential and opens a new avenue for the inclusion of
405 the microbiome in the future ecosystem health assessments. This study introduces a new basis for the future
406 development of the specific methods and tools to analyse the interactions existing between nematodes and
407 microbiome as well as understanding the role that microbiome has in mediating the sediment-nematodes
408 relationship in marine benthic ecosystems.

409

410

411 **Statements & Declarations**

412

413 **Acknowledgements**

414 The authors would like to thank the help from Jordana Branco in the sample collection.

415

416 **Funding**

417 This work was supported by national funds through Fundação para a Ciência e Tecnologia (FCT): D4Ss
418 (ALT20-03-0145-FEDER-029400); UIDB/04292/2020-MARE; NIPOGES (MAR-01.03.02-FEAMP-
419 0013); AQUASADO (MAR-02.01.01-FEAMP-0051); COASTNET (PINFRA/22128/2016) and
420 MINEPLAT (ALT20030145- FEDER000013). SV was supported by FCT PhD Fellowship
421 2021.06804.BD.

422

423 **Author Contributions**

424 Cláudia S. L. Vicente and Helena Adão contributed to the study conception and design. All authors
425 contributed for the sampling collections. Sediment analysis were performed by Joana Neves, Marta Martins
426 and Helena Costa. Data collection and analysis were performed by Soraia Vieira, Kasia Sroczynska, Helena
427 Adão and Cláudia S. L. Vicente. The first draft of the manuscript was written by Soraia Vieira, and all
428 authors commented on previous versions of the manuscript. All authors read and approved the final
429 manuscript.

430

431 **Data Availability**

432 The data sets generated and analysed during the current study are available in NCBI SRA repository under
433 the Bioproject PRJNA680980 (<https://www.ncbi.nlm.nih.gov/bioproject/?term=PRJNA680980>) and
434 accessions SRR13151077-13151079 (NAV), SRR13165305-13165307 (TRO), and SRR13165323-
435 SRR13165325 (MOI).

436

437 **Code availability**

438 Not applicable.

439

440 **Ethics declarations**

441 Not applicable

442

443 **Consent for publication**

444 Not applicable

445

446 **Conflict of interest**

447 The authors declare no competing interests.

448

449

450 **References**

- 451 1. Bonaglia S, Nascimento FJA, Bartoli M, et al (2014) Meiofauna increases bacterial denitrification
452 in marine sediments. <https://doi.org/10.1038/ncomms6133>
- 453 2. Schratzberger M, Ingels J (2018) Meiofauna matters: The roles of meiofauna in benthic ecosystems.
454 J Exp Mar Bio Ecol 502:12–25. <https://doi.org/10.1016/j.jembe.2017.01.007>
- 455 3. Schratzberger M, Somerfield PJ (2020) Effects of widespread human disturbances in the marine
456 environment suggest a new agenda for meiofauna research is needed. Sci. Total Environ.
457 728:138435
- 458 4. Semprucci F, Balsamo M (2014) Free-Living Marine Nematodes as Bioindicators: Past, Present
459 and Future Perspectives. Trends Environ Sci 17–36
- 460 5. Schratzberger M, Warwick R (1998) Effects of the intensity and frequency of organic enrichment
461 on two estuarine nematode communities. Mar Ecol Prog Ser 164:83–94.
462 <https://doi.org/10.3354/meps164083>
- 463 6. Ridall A, Ingels J (2021) Suitability of Free-Living Marine Nematodes as Bioindicators: Status
464 and Future Considerations. Front Mar Sci 0:863. <https://doi.org/10.3389/FMARS.2021.685327>
- 465 7. Nascimento FJA, Näslund J, Elmgren R (2012) Meiofauna enhances organic matter mineralization
466 in soft sediment ecosystems. Limnol Oceanogr 57:338–346.
467 <https://doi.org/10.4319/lo.2012.57.1.0338>
- 468 8. Derycke S, De Meester N, Rigaux A, et al (2016) Coexisting cryptic species of the *Litoditis marina*
469 complex (Nematoda) show differential resource use and have distinct microbiomes with high
470 intraspecific variability. Mol Ecol 25:2093–2110. <https://doi.org/10.1111/mec.13597>
- 471 9. Moens T, Bouillon S, Gallucci F (2005) Dual stable isotope abundances unravel trophic position
472 of estuarine nematodes. J Mar Biol Assoc United Kingdom 85:1401–1407.
473 <https://doi.org/10.1017/S0025315405012580>
- 474 10. De Mesel I, Derycke S, Swings J, et al (2006) Role of nematodes in decomposition processes: Does
475 within-trophic group diversity matter? Mar Ecol Prog Ser 321:157–166.
476 <https://doi.org/10.3354/meps321157>
- 477 11. D’Hondt AS, Stock W, Blommaert L, et al (2018) Nematodes stimulate biomass accumulation in
478 a multispecies diatom biofilm. Mar Environ Res 140:78–89.
479 <https://doi.org/10.1016/j.marenvres.2018.06.005>

- 480 12. Vafeiadou A-MM, Materatski P, Adão H, et al (2013) Food sources of macrobenthos in an estuarine
481 seagrass habitat (*Zostera noltii*) as revealed by dual stable isotope signatures. *Mar Biol* 160:2517–
482 2523. <https://doi.org/10.1007/s00227-013-2238-0>
- 483 13. Moens T, Vafeiadou AM, De Geyter E, et al (2014) Diatom feeding across trophic guilds in tidal
484 flat nematodes, and the importance of diatom cell size. *J Sea Res* 92:125–133.
485 <https://doi.org/10.1016/j.seares.2013.08.007>
- 486 14. Van der Heijden LH, Graeve M, Asmus R, et al (2019) Trophic importance of microphytobenthos
487 and bacteria to meiofauna in soft-bottom intertidal habitats: A combined trophic marker approach.
488 *Mar Environ Res* 149:50–66. <https://doi.org/10.1016/j.marenvres.2019.05.014>
- 489 15. Hargrave BT, Holmer M, Newcombe CP (2008) Towards a classification of organic enrichment in
490 marine sediments based on biogeochemical indicators. *Mar Pollut Bull* 56:810–824.
491 <https://doi.org/10.1016/J.MARPOLBUL.2008.02.006>
- 492 16. Wang W, Tao J, Liu H, et al (2020) Contrasting bacterial and archaeal distributions reflecting
493 different geochemical processes in a sediment core from the Pearl River Estuary. *AMB Express*
494 10:1–14. <https://doi.org/10.1186/s13568-020-0950-y>
- 495 17. Bayer C, Heindl NR, Rinke C, et al (2009) Molecular characterization of the symbionts associated
496 with marine nematodes of the genus *Robbea*. *Environ Microbiol Rep* 1:136–144.
497 <https://doi.org/10.1111/j.1758-2229.2009.00019.x>
- 498 18. Broman E, Bonaglia S, Holovachov O, et al (2020) Uncovering diversity and metabolic spectrum
499 of animals in dead zone sediments. *Commun Biol* 3:1–12. [https://doi.org/10.1038/s42003-020-](https://doi.org/10.1038/s42003-020-0822-7)
500 0822-7
- 501 19. Materatski P, Vafeiadou A-MM, Ribeiro R, et al (2015) A comparative analysis of benthic
502 nematode assemblages from *Zostera noltii* beds before and after a major vegetation collapse. *Estuar*
503 *Coast Shelf Sci* 167:256–268. <https://doi.org/10.1016/j.ecss.2015.07.001>
- 504 20. Branco J, Pedro S, Alves AS, et al (2018) Natural recovery of *Zostera noltii* seagrass beds and
505 benthic nematode assemblage responses to physical disturbance caused by traditional harvesting
506 activities. *J Exp Mar Bio Ecol* 502:191–202. <https://doi.org/10.1016/J.JEMBE.2017.03.003>
- 507 21. Bulseco AN, Vineis JH, Murphy AE, et al (2020) Metagenomics coupled with biogeochemical
508 rates measurements provide evidence that nitrate addition stimulates respiration in salt marsh
509 sediments. *Limnol Oceanogr* 65:S321–S339. <https://doi.org/10.1002/lno.11326>

- 510 22. De Bettencourt AM, Bricker S, Marques JC, Joanaz De Melo J (2003) Typology and Reference
511 Conditions for Portuguese Transitional and Coastal Waters, Development of guidelines for the
512 application of the European Union Water Framework Directive. TIC... Fatty Acids as
513 Bioindicators View project DEVOTES: DEvelopment Of innovative Tools for understanding
514 marine biodiversity and assessing View project
- 515 23. Lillebø AI, Coelho PJ, Pato P, et al (2011) Assessment of Mercury in Water, Sediments and Biota
516 of a Southern European Estuary (Sado Estuary, Portugal). *Water, Air, Soil Pollut* 214:667–680.
517 <https://doi.org/10.1007/s11270-010-0457-2>
- 518 24. Caeiro S, Costa MH, Ramos TB, et al (2005) Assessing heavy metal contamination in Sado
519 Estuary sediment: An index analysis approach. *Ecol Indic* 5:151–169.
520 <https://doi.org/https://doi.org/10.1016/j.ecolind.2005.02.001>
- 521 25. Caeiro S, Costa MH, DeIvalls A, et al (2009) Ecological risk assessment of sediment
522 management areas: application to Sado Estuary, Portugal. *Ecotoxicology* 18:1165–1175.
523 <https://doi.org/10.1007/s10646-009-0372-8>
- 524 26. Sroczyńska K, Chainho P, Vieira S, Adão H (2021) What makes a better indicator? Taxonomic vs
525 functional response of nematodes to estuarine gradient. *Ecol Indic* 121:107113.
526 <https://doi.org/10.1016/j.ecolind.2020.107113>
- 527 27. Sroczyńska K, Conde A, Chainho P, Adão H (2021) How nematode morphometric attributes
528 integrate with taxonomy-based measures along an estuarine gradient. *Ecol Indic* 124:107384.
529 <https://doi.org/10.1016/j.ecolind.2021.107384>
- 530 28. Caporaso JG, Lauber CL, Walters WA, et al (2012) Ultra-high-throughput microbial community
531 analysis on the Illumina HiSeq and MiSeq platforms. *ISME J* 6:1621–1624.
532 <https://doi.org/10.1038/ismej.2012.8>
- 533 29. Bolyen E, Rideout JR, Dillon MR, et al (2019) QIIME 2: Reproducible, interactive, scalable, and
534 extensible microbiome data science. <https://doi.org/10.7287/peerj.preprints.27295v2>
- 535 30. Callahan BJ, McMurdie PJ, Rosen MJ, et al (2016) DADA2: High-resolution sample inference
536 from Illumina amplicon data. *Nat Methods* 2016 137 13:581–583.
537 <https://doi.org/10.1038/nmeth.3869>
538
539

- 540 31. Quast C, Pruesse E, Yilmaz P, et al (2013) The SILVA ribosomal RNA gene database project:
541 improved data processing and web-based tools. *Nucleic Acids Res* 41:D590–D596.
542 <https://doi.org/10.1093/NAR/GKS1219>
- 543 32. Bokulich N, Robeson M, Dillon M, et al (2021) bokulich-lab/RESCRIPT: 2021.8.0.dev0.
544 <https://doi.org/10.5281/ZENODO.4811136>
- 545 33. Heip C, Vincx M, Vranken G (1985) *The ecology of marine nematodes*
- 546 34. Vincx M (1996) Meiofauna in marine and freshwater sediments. In: *Meiofauna in marine and*
547 *freshwater sediments*. In Hall G.S. (ed.) *Methods for the Examination of Organismal Diversity in*
548 *Soils and Sediments*, Wallingford, UK. pp 187–195
- 549 35. Platt H, Warwick R (1983) *Freeliving marine nematodes. Part 1: British enoplids. Pictorial key to*
550 *world genera and notes for the identification of British species.*
- 551 36. Warwick RM, Platt HM, Sommerfield PJ (1998) *Free-living marine nematodes, Part 3, British*
552 *Monhysterids*. Field Studies Council, Shrewsbury
- 553 37. Bezerra TN, Eisendle U, Hodda M, et al (2021) Nemys: World Database of Nematodes.
554 *Anisakidae* Railliet & Henry, 1912. <http://nemys.ugent.be/aphia.php?p=taxdetails&id=19961>.
555 Accessed 29 Sep 2021
- 556 38. Clarke K, interpretation RW statistical analysis and, 2001 undefined (2001) *Change in marine*
557 *communities*. researchgate.net
- 558 39. Anderson MJ, Gorley RN, Clarke KR (2008) PERMANOVA+ for PRIMER: Guide to Software
559 and Statistical Methods. In: Plymouth, UK
- 560 40. McMurdie PJ, Holmes S (2013) phyloseq: An R Package for Reproducible Interactive Analysis
561 and Graphics of Microbiome Census Data. *PLoS One* 8:e61217.
562 <https://doi.org/10.1371/JOURNAL.PONE.0061217>
- 563 41. Legendre P, Gallagher ED (2001) Ecologically meaningful transformations for ordination of
564 species data. *Oecologia* 129:271–280. <https://doi.org/10.1007/s004420100716>
- 565 42. R Core Team (2012) *R: A language and environment for statistical computing*
- 566 43. Kindt R, Coe R (2005) *Tree Diversity Analysis. A manual and software for common statistical*
567 *methods and biodiversity studies*. <https://doi.org/10.13140/RG.2.1.1993.7684>
- 568 44. Jackson DA (1995) PROTEST: A PROcrustean Randomization TEST of community
569 environment concordance. *Ecoscience* 2:297–303.

- 570 <https://doi.org/10.1080/11956860.1995.11682297>
- 571 45. Peres-Neto PR, Jackson DA (2001) How well do multivariate data sets match? The advantages of
572 a Procrustean superimposition approach over the Mantel test. *Oecologia* 2001 1292 129:169–178.
573 <https://doi.org/10.1007/S004420100720>
- 574 46. Margalef R (1958) Information theory in ecology, 3rd ed. General Systems
- 575 47. Shannon, C.E.; Weaver W (1963) The Mathematical Theory of Communication. Univ Illinois Press
576 Illinois
- 577 48. Bongers T, Alkemade R, Yeates GW, Bongers, T., Alkemade, R. YWG (1991) Interpretation of
578 disturbance-induced maturity decrease in marine nematode assemblages by means of the Maturity
579 Index
- 580 49. Bongers T (1990) *Oecologia* The maturity index: an ecological measure of environmental
581 disturbance based on nematode species composition
- 582 50. Wieser W (1956) Some free-living marine nematodes. *Galathea Rep*
- 583 51. Herlemann DPR, Labrenz M, Jürgens K, et al (2011) Transitions in bacterial communities along
584 the 2000 km salinity gradient of the Baltic Sea. *ISME J* 5:1571–1579.
585 <https://doi.org/10.1038/ismej.2011.41>
- 586 52. Jessen GL, Lichtschlag A, Ramette A, et al (2017) Hypoxia causes preservation of labile organic
587 matter and changes seafloor microbial community composition (Black Sea). *Sci Adv* 3:e1601897.
588 <https://doi.org/10.1126/sciadv.1601897>
- 589 53. Baker BJ, Lazar CS, Teske AP, Dick GJ (2015) Genomic resolution of linkages in carbon, nitrogen,
590 and sulfur cycling among widespread estuary sediment bacteria. [https://doi.org/10.1186/s40168-](https://doi.org/10.1186/s40168-015-0077-6)
591 [015-0077-6](https://doi.org/10.1186/s40168-015-0077-6)
- 592 54. Raggi L, García-Guevara F, Godoy-Lozano EE, et al (2020) Metagenomic Profiling and Microbial
593 Metabolic Potential of Perdido Fold Belt (NW) and Campeche Knolls (SE) in the Gulf of Mexico.
594 *Front Microbiol* 11:1825. <https://doi.org/10.3389/fmicb.2020.01825>
- 595 55. Spring S, Scheuner C, Göker M, Klenk H-P (2015) A taxonomic framework for emerging groups
596 of ecologically important marine gammaproteobacteria based on the reconstruction of evolutionary
597 relationships using genome-scale data. *Front Microbiol* 0:281.
598 <https://doi.org/10.3389/FMICB.2015.00281>
- 599 56. Marshall A, Longmore A, Phillips L, et al (2021) Nitrogen cycling in coastal sediment microbial

- 600 communities with seasonally variable benthic nutrient fluxes. *Aquat Microb Ecol* 86:1–19.
601 <https://doi.org/10.3354/ame01954>
- 602 57. Ott J, Bright M, Bulgheresi SV (2004) Symbioses between Marine Nematodes and Sulfur-oxidizing
603 Chemoautotrophic Bacteria
- 604 58. Zimmermann J, Wentrup C, Sadowski M, et al (2016) Closely coupled evolutionary history of ecto-
605 and endosymbionts from two distantly related animal phyla. *Mol Ecol* 25:3203–3223.
606 <https://doi.org/10.1111/mec.13554>
- 607 59. Wunder LC, Aromokeye DA, Yin X, et al (2021) Iron and sulfate reduction structure microbial
608 communities in (sub-)Antarctic sediments. *ISME J* 15:3587–3604. [https://doi.org/10.1038/s41396-](https://doi.org/10.1038/s41396-021-01014-9)
609 [021-01014-9](https://doi.org/10.1038/s41396-021-01014-9)
- 610 60. Kolda A, Ljubešić Z, Gavrilović A, et al (2020) Metabarcoding Cyanobacteria in coastal waters
611 and sediment in central and southern Adriatic Sea. *hrca.hr* 79:157–169.
612 <https://doi.org/10.37427/botcro-2020-021>
- 613 61. Waite DW, Chuvochina M, Pelikan C, et al (2020) Proposal to reclassify the proteobacterial classes
614 Deltaproteobacteria and Oligoflexia, and the phylum Thermodesulfobacteria into four phyla
615 reflecting major functional capabilities. *Int J Syst Evol Microbiol* 70:5972–6016.
616 <https://doi.org/10.1099/ijsem.0.004213>
- 617 62. Alves ASS, Adão H, Ferrero TJJ, et al (2013) Benthic meiofauna as indicator of ecological changes
618 in estuarine ecosystems: The use of nematodes in ecological quality assessment. *Ecol Indic* 24:462–
619 475. <https://doi.org/10.1016/J.ECOLIND.2012.07.013>
- 620 63. Adão H, Alves AS, Patrício J, et al (2009) Spatial distribution of subtidal Nematoda communities
621 along the salinity gradient in southern European estuaries. *Acta Oecologica* 35:287–300.
622 <https://doi.org/10.1016/j.actao.2008.11.007>
- 623 64. Steyaert M, Vanaverbeke J, Vanreusel A, et al (2003) The importance of fine-scale, vertical profiles
624 in characterising nematode community structure. *Estuar Coast Shelf Sci* 58:353–366.
625 [https://doi.org/10.1016/S0272-7714\(03\)00086-6](https://doi.org/10.1016/S0272-7714(03)00086-6)
- 626 65. Alves AS, Adão H, Patrício J, et al (2009) Spatial distribution of subtidal meiobenthos along
627 estuarine gradients in two southern european estuaries (Portugal). *J Mar Biol Assoc United*
628 *Kingdom* 89:1529–1540. <https://doi.org/10.1017/S0025315409000691>
- 629 66. Ecol Prog Ser Paul Montagna MA (1984) In situ measurement of meiobenthic grazing rates on

- 630 sediment bacteria and edaphic diatoms* MARINE ECOLOGY-PROGRESS SERIES
- 631 67. Sahraean N, Bezerra TC, Ejlali Khanaghah K, et al (2017) Effects of pollution on nematode
632 assemblage structure and diversity on beaches of the northern Persian Gulf. *Hydrobiologia*
633 799:349–369.
- 634 68. Schuelke, T., Pereira, T.J., Hardy, S.M., Bik, H.M. (2018) Nematode-associated microbial taxa do
635 not correlate with host phylogeny, geographic region or feeding morphology in marine sediment
636 habitats. *Mol Ecol* 27: 1930–1951.
- 637
- 638
- 639

640 **Figures captions**

641

642 **Figure 1.** Sado estuary located at Southwest of Portugal (38° 31' 14" N, 8° 53' 32" W). The selected
643 sampling sites: Navigator (38.487033, -8.795686) (grey circle), highly industrialized area; Moinho
644 (38.528101, -8.802995) (orange circle) with high organic inputs and Tróia (38.417317, -8.816433) (green
645 circle) with coarser sediment. Moinho and Tróia are situated in a protected area

646

647 **Figure 2.** Principal component analysis, based on Bray-Curtis Distances, according to environmental
648 variables measured (OM, gravel, sand, FF, IN, IC CO and salinity) at each sampling site: Navigator,
649 Moinho and Troia, PC1 59.2%; PC2 31.4%

650

651 **Figure 3.** Principal component analysis, based on Bray-Curtis Distances, according to OTUs relative
652 abundance of genera level obtained in each "site". PC1 = 32.6 % and PC2 =17.4 %. The vectors are the
653 most representative genera of the variability observed in bacterial communities

654

655 **Figure 4.** Bar plot displays the relative abundance of OTUs (%), based Phylum-level, that represents more
656 than 90% of the total abundance in each site Moinho (MOI); Navigator (NAV) and Tróia (TROIA), n=3,
657 the relative frequencies smaller than 1% collapsed into the N/A category

658

659 **Figure 5.** Bar plot displays the highest density of nematodes genera which represents 90% of the total
660 abundance in each sampling site Moinho (MOIRn), Navigator (NAVRn) and Tróia (TROIARn),
661 Replicates, n=1,2,3

662

663 **Figure 6.** Principal component analysis, based on Bray-Curtis Distances, according to nematode density at
664 Genus-level in each "sites" Moinho, Navigator and Tróia. PC1 = 40.9 % and PC2 =25 %. The vectors
665 represent the genera highest variability of the nematode assemblages

666

667 **Figure 7.** Constrained redundancy analysis displaying contributions of environmental factors to (A)
668 bacterial composition (RDA1= 66.9% and RDA2 = 14.7%) and (B) nematode assemblages (RDA1= 36.5%
669 and RDA2 = 24.5%)

671 **Tables**

672

673 **Table 1.** One-way PERMANOVA test, Beta-diversity of bacterial communities, between "Sites" (3 level
674 fixed) for all variables analysed, ($p \leq 0.05$), $n=3$

	<i>Degree of freedom</i>	<i>Sum squares</i>	<i>Mean square</i>	<i>Pseudo-F</i>	<i>P(perm)</i>	<i>Unique perms</i>	<i>P(MC)</i>
<i>Bacterial abundance</i>	2	1108.3	554.13	1.7106	0.007	280	0.0983
	6	1943.7	323.95				
	8	3052					

675

676 **Table 2.** Mean density \pm standard error (SE) of the nematode genera (number of individuals per 10 cm⁻²),
677 at each sampling site (Moinho, Navigator and Tróia). Trophic group (TG) and *c-p* value of each genera
678 included. Only the most abundant genera are included in this table

679

<i>Genera</i>	<i>TG</i>	<i>cp-value</i>	<i>Moinho</i>	<i>Navigator</i>	<i>Tróia</i>
<i>Metachromadora</i>	2B	2	7557.7 \pm 803	412.8 \pm 127	1872.5 \pm 249
<i>Terschellingia</i>	1A	3	1868.2 \pm 777	1413.8 \pm 844	613.6 \pm 111
<i>Sabatieria</i>	1B	2	1146.1 \pm 653	256.2 \pm 40	285.4 \pm 50
<i>Axonolaimus</i>	1B	2	733.8 \pm 294	12.5 \pm 6	68.4 \pm 11
<i>Sphaerolaimus</i>	2B	3	730.9 \pm 410	45.7 \pm 6	42.1 \pm 4
<i>Ptycholaimellus</i>	2A	3	371.4 \pm 113	19 \pm 7	286.2 \pm 212
<i>Anoplostoma</i>	1B	2	204.7 \pm 94	131.5 \pm 44	95.6 \pm 56
<i>Daptonema</i>	1B	2	169.7 \pm 68	23.8 \pm 11	16.3 \pm 12
<i>Daptonema spl</i>	1B	2	149.1 \pm 115	28.5 \pm 9	59 \pm 34
<i>Spilophorella</i>	2A	2	99.4 \pm 77	0	7.9 \pm 6
<i>Microlaimus</i>	2A	2	64.1 \pm 49	52 \pm 40	29.7 \pm 23

<i>Comesoma</i>	1B	2	49.7 ± 38	3.2 ± 2	0
<i>Dichromadora</i>	2A	2	49.7 ± 38	7.9 ± 3	49.1 ± 38
<i>Oncholaimellus</i>	2B	3	49.7 ± 38	27.8 ± 21	0
<i>Praeacanthonchus</i>	2A	4	49.7 ± 38	3.3 ± 2	24.3 ± 10
<i>Anticoma</i>	1A	2	35.1 ± 27	0	0
<i>Cyatholaimus</i>	2A	2	35.1 ± 27	27.1 ± 11	0
<i>Prochromadorella</i>	2A	2	35.1 ± 27	0	0
<i>Viscosia</i>	2B	3	35.1 ± 27	34.9 ± 13	73.4 ± 47
<i>Total</i>			13466.8 ± 3745	2706.3 ± 1304	3842.8 ± 1036

680

Figures

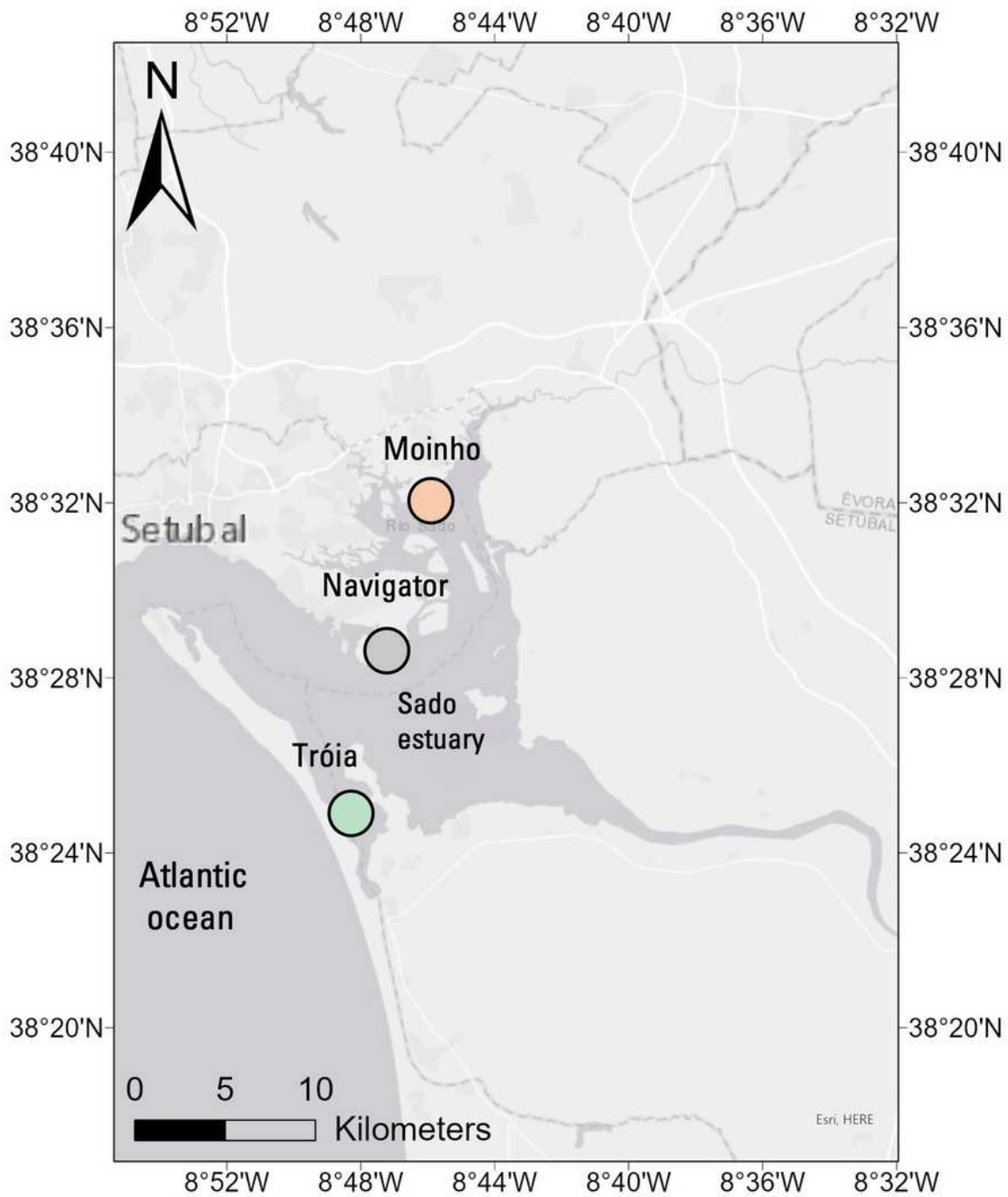


Figure 1

Sado estuary located at Southwest of Portugal (38° 31' 14" N, 8° 53' 32" W). The selected sampling sites: Navigator (38.487033, -8.795686) (grey circle), highly industrialized area; Moinho (38.528101, -8.802995)

(orange circle) with high organic inputs and Tróia (38.417317, -8.816433) (green circle) with coarser sediment. Moinho and Tróia are situated in a protected area

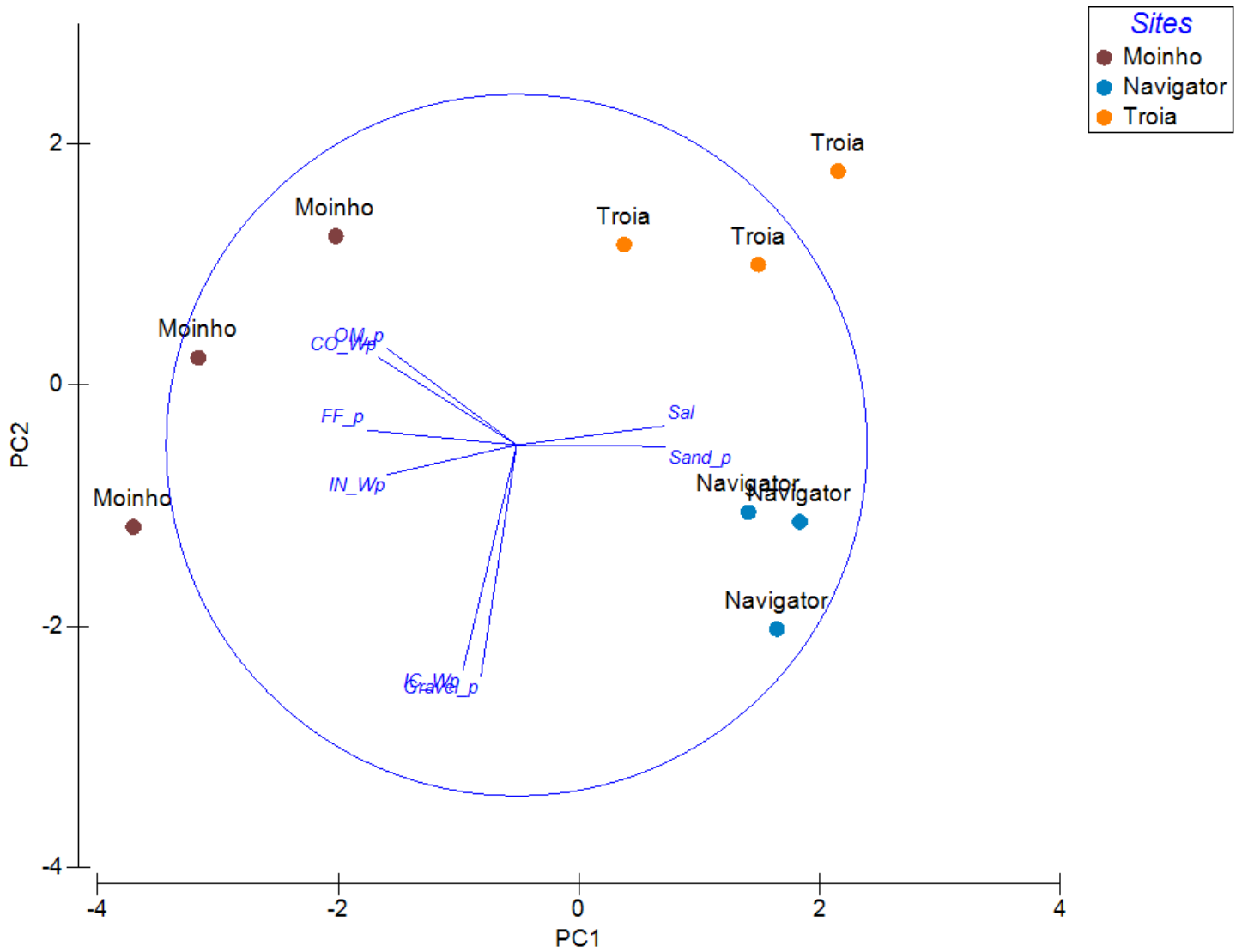


Figure 2

Principal component analysis, based on Bray-Curtis Distances, according to environmental variables measured (OM, gravel, sand, FF, IN, IC CO and salinity) at each sampling site: Navigator, Moinho and Troia, PC1 59.2%; PC2 31.4%

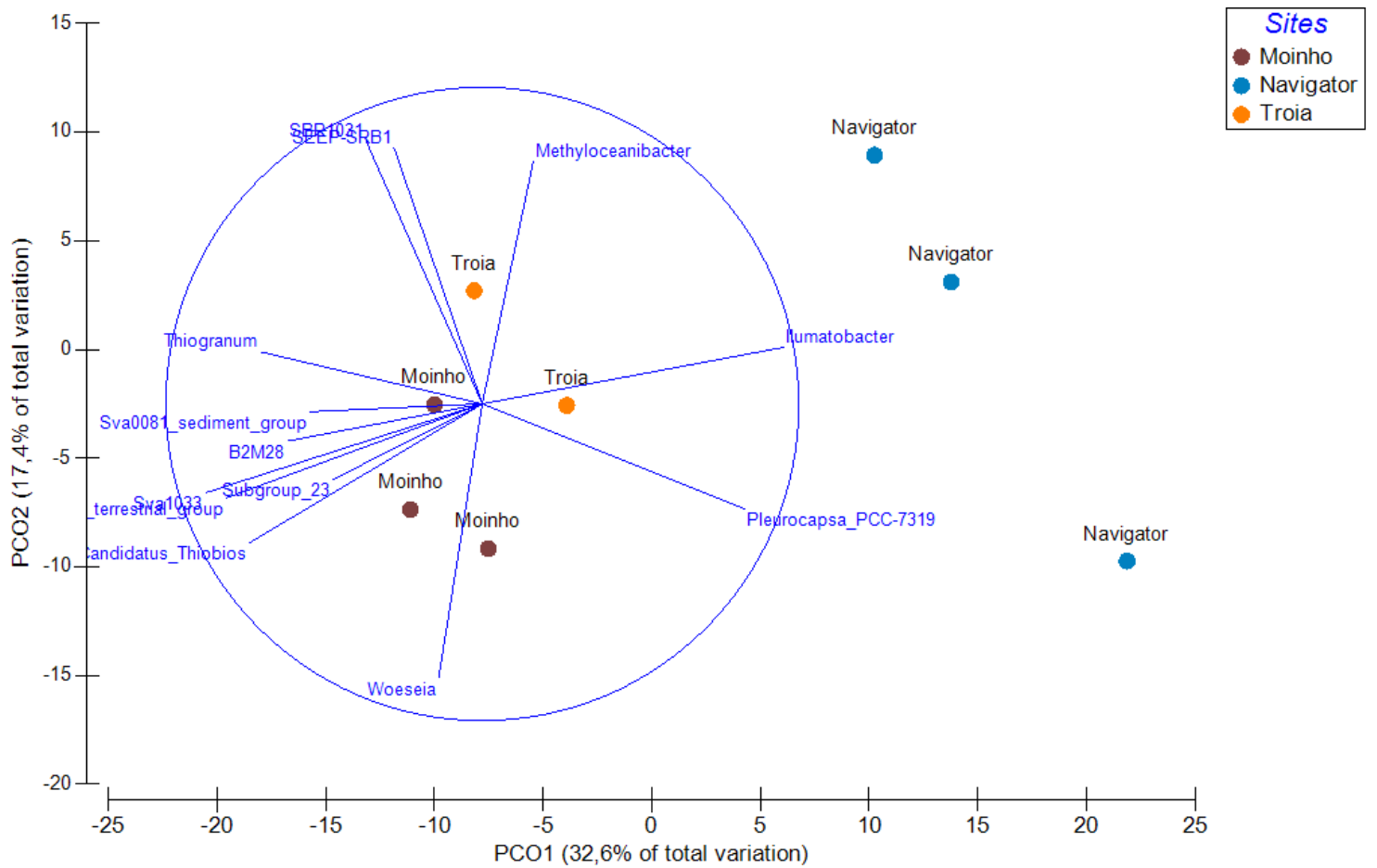


Figure 3

Principal component analysis, based on Bray-Curtis Distances, according to OTUs relative abundance of genera level obtained in each "site". PC1 = 32.6 % and PC2 = 17.4 %. The vectors are the most representative genera of the variability observed in bacterial communities

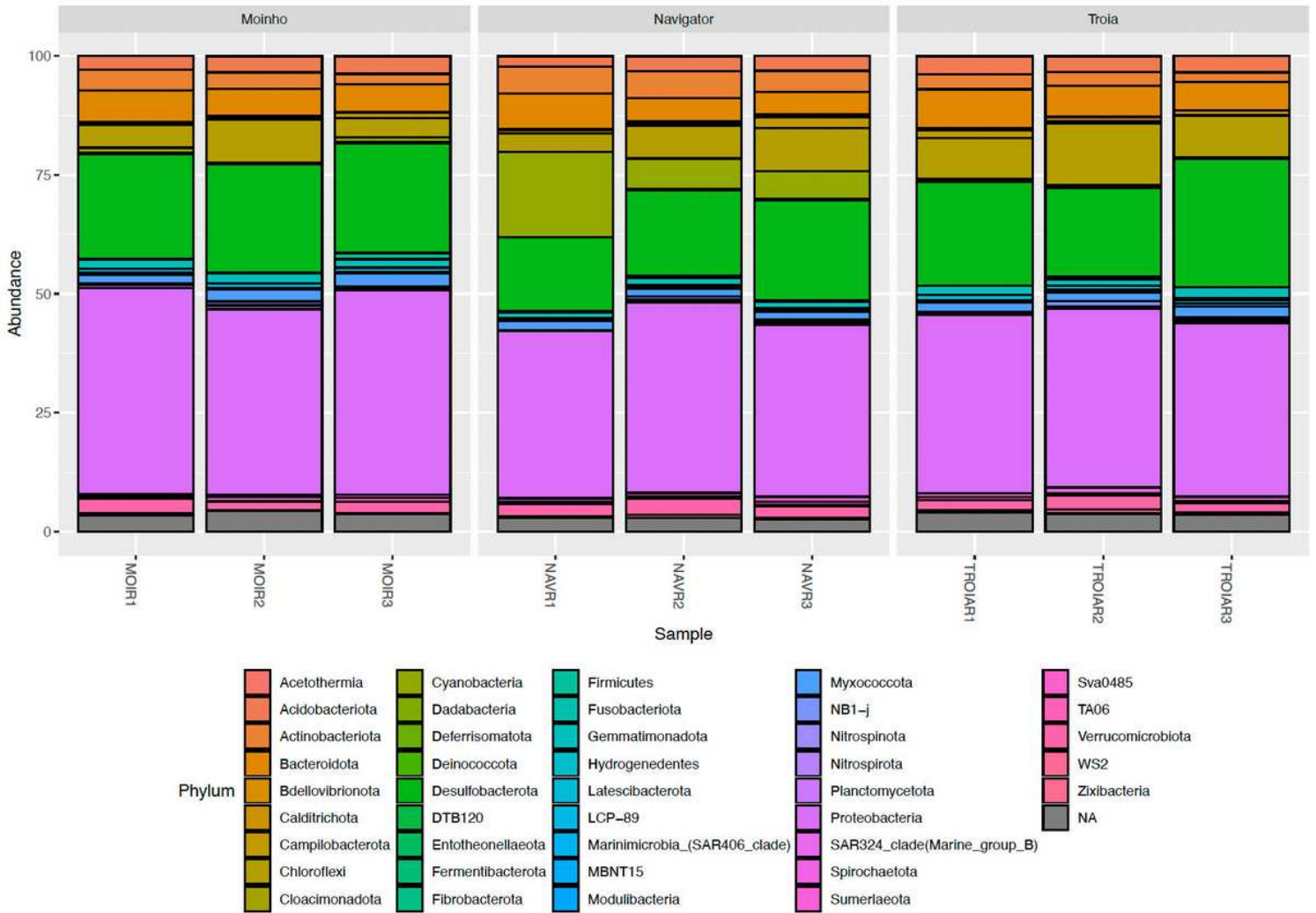


Figure 4

Bar plot displays the relative abundance of OTUs (%), based Phylum-level, that represents more than 90% of the total abundance in each site Moinho (MOI); Navigator (NAV) and Tróia (TROI), n=3, the relative frequencies smaller than 1% collapsed into the N/A category

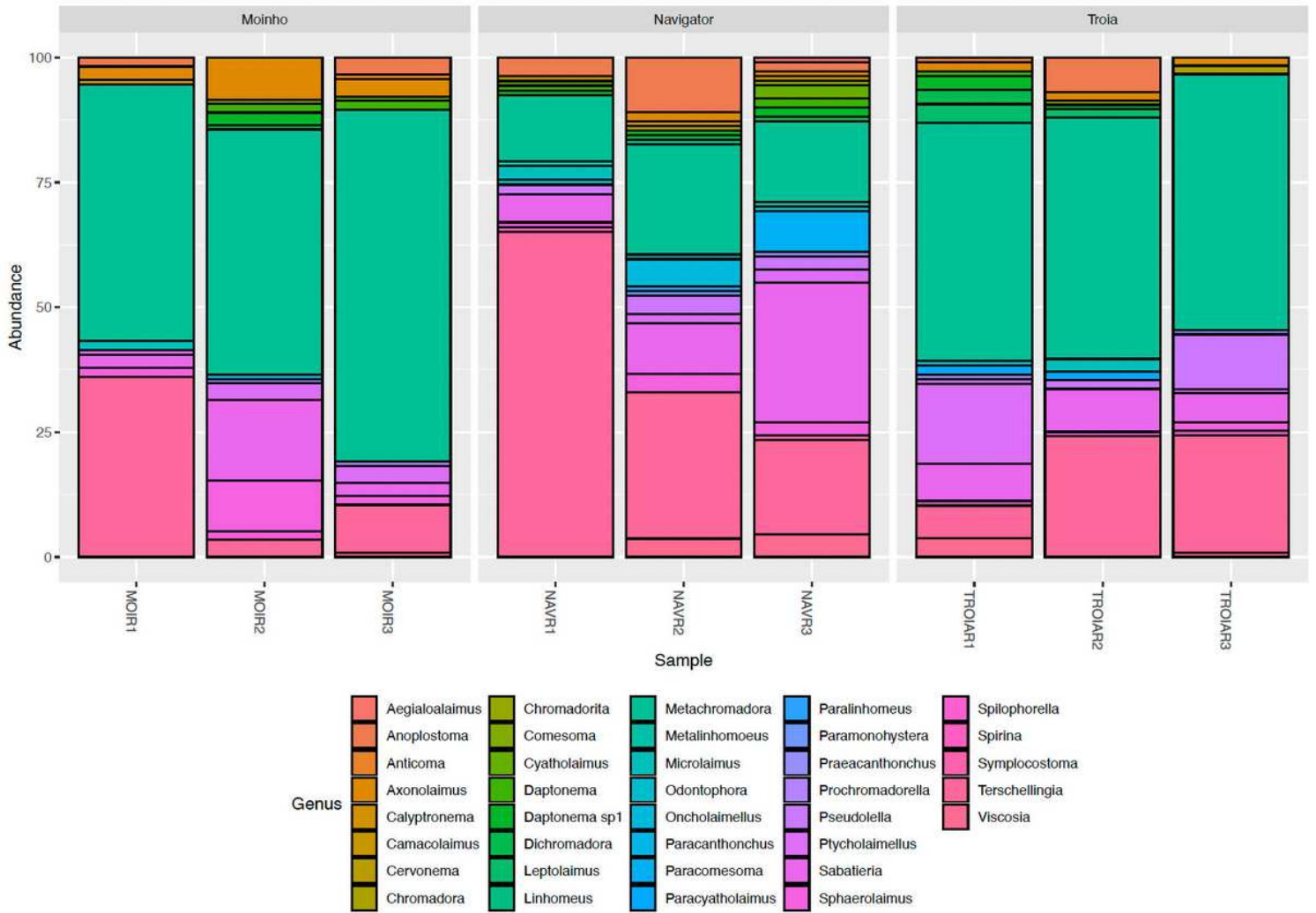


Figure 5

Bar plot displays the highest density of nematodes genera which represents 90% of the total abundance in each sampling site Moinho (MOIRn), Navigator (NAVRn) and Tróia (TROIARn), Replicates, n=1,2,3

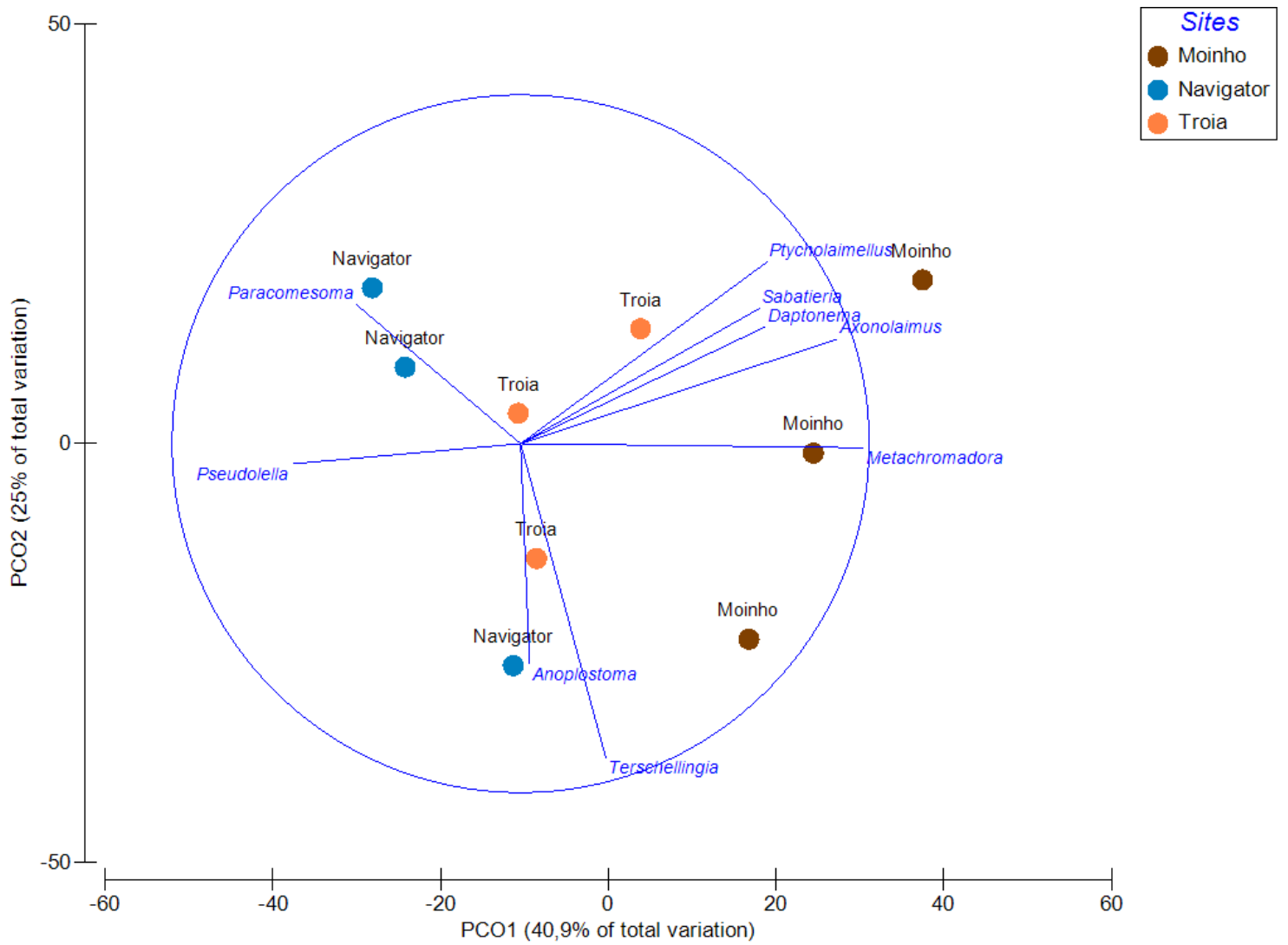
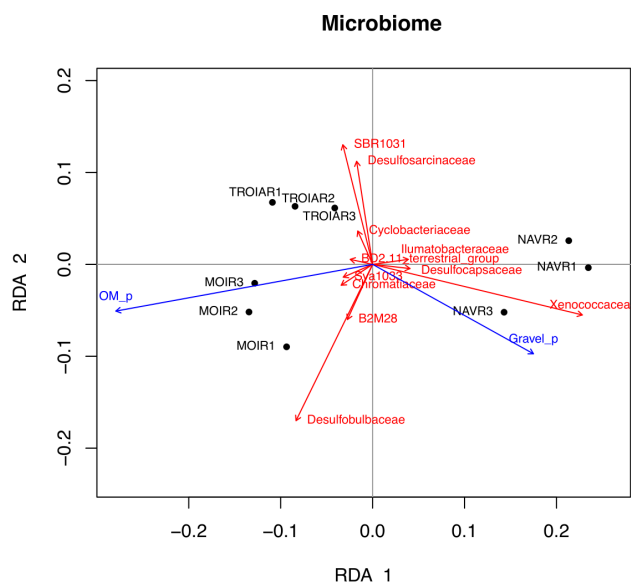
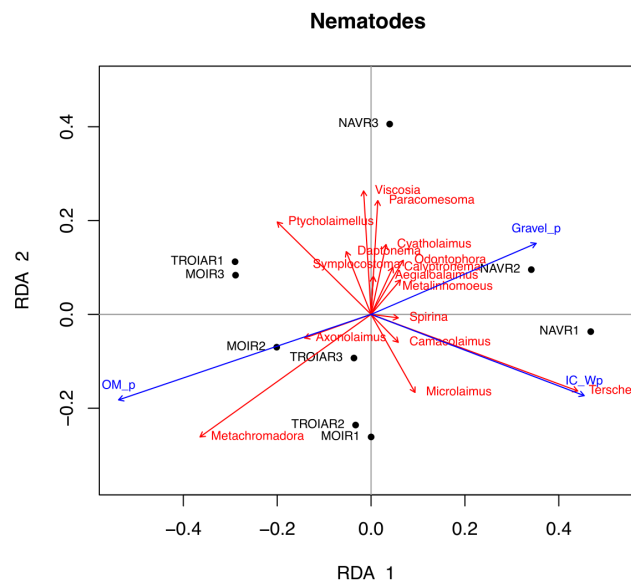


Figure 6

Principal component analysis, based on Bray-Curtis Distances, according to nematode density at Genus-level in each "sites" Moinho, Navigator and Tróia. PC1 = 40.9 % and PC2 =25 %. The vectors represent the genera highest variability of the nematode assemblages



A



B

Figure 7

Constrained redundancy analysis displaying contributions of environmental factors to (A) bacterial composition (RDA1= 66.9% and RDA2 = 14.7%) and (B) nematode assemblages (RDA1= 36.5% and RDA2 = 24.5%)

Supplementary Files

This is a list of supplementary files associated with this preprint. Click to download.

- [SupplementaryTablesandFigures.docx](#)